

Towards Dynamic Trend Filtering through Trend Point Detection with Reinforcement Learning

Jihyeon Seong¹, Sekwang Oh¹ and Jaesik Choi^{1,2}

¹Korea Advanced Institute of Science and Technology (KAIST), South Korea

²INEEJI, South Korea

{jihyeon.seong, oskoskosk, jaesik.choi}@kaist.ac.kr,

Abstract

Trend filtering simplifies complex time series data by applying smoothness to filter out noise while emphasizing proximity to the original data. However, existing trend filtering methods fail to reflect abrupt changes in the trend due to ‘approximate-ness,’ resulting in constant smoothness. This approximateness uniformly filters out the tail distribution of time series data, characterized by extreme values, including both abrupt changes and noise. In this paper, we propose Trend Point Detection formulated as a Markov Decision Process (MDP), a novel approach to identifying essential points that should be reflected in the trend, departing from approximations. We term these essential points as Dynamic Trend Points (DTPs) and extract trends by interpolating them. To identify DTPs, we utilize Reinforcement Learning (RL) within a discrete action space and a forecasting sum-of-squares loss function as a reward, referred to as the Dynamic Trend Filtering network (DTF-net). DTF-net integrates flexible noise filtering, preserving critical original subsequences while removing noise as required for other subsequences. We demonstrate that DTF-net excels at capturing abrupt changes compared to other trend filtering algorithms and enhances forecasting performance, as abrupt changes are predicted rather than smoothed out.

1 Introduction

Trend filtering emphasizes proximity to the original time series data while filtering out noise through smoothness [Leser, 1961]. Smoothness in trend filtering simplifies complex patterns within noisy and non-stationary time series data, making it effective for forecasting and anomaly detection [Park *et al.*, 2020]. While smoothness achieves the property of noise filtering, an ‘abrupt change’ denotes a point in a time series where the trend experiences a sharp transition, signaling a change in slope. Given that abrupt changes determine the direction and persistence of the slope, it is crucial to incorporate them into the trend. Traditional trend filtering employs a sum-of-squares function to reflect abrupt changes while utilizing second-order differences as a regularization

term to attain smoothness [Hodrick and Prescott, 1997; Kim *et al.*, 2009]. However, we found that the constant nature of smoothness filters out abrupt changes, making it challenging to distinguish them from noise.

The issue of constant smoothness arises from the reliance on the property of ‘approximate-ness.’ Evidence presented by [Ding *et al.*, 2019] suggests that the sum-of-squares function eliminates tail distribution as outliers since it approximates a Gaussian distribution with a light-tail shape. As both abrupt changes and noise reside within the tail distribution, filtering out only noise becomes challenging. This uniform filtering results in the loss of valuable abrupt changes that should be reflected in the trend [Wen *et al.*, 2019].

In this paper, we propose Trend Point Detection formulated as a Markov Decision Process (MDP), aiming to identify essential points that should be reflected in the trend, departing from approximateness [Sutton and Barto, 2018]. These essential points are termed Dynamic Trend Points (DTPs), and trends are extracted by interpolating them. We utilize the Reinforcement Learning (RL) algorithm within a discrete action space to solve the MDP problem, referred to as a Dynamic Trend Filtering network (DTF-net) [Schulman *et al.*, 2017]. RL can directly detect essential points through an agent without being constrained by fixed window sizes or frequencies within the time series data domain. This dynamic approach enables the adjustment of noise filtering levels for each subsequence within the time series.

Building on prior research regarding reward function learning based on Gaussian Process (GP) [Biyik *et al.*, 2020], we define the reward function as the sum-of-squares loss function from Time Series Forecasting (TSF). This choice is supported by [Ding *et al.*, 2019], which suggests that the sum-of-squares function approximates a Gaussian distribution and functions similarly to a Gaussian kernel. Note that using a Gaussian kernel function as a reward leverages RL to effectively optimize the agent while learning the full distribution of time series data. Through the TSF reward, temporal dependencies around DTPs can be captured, and the level of smoothness is controlled by adjusting the forecasting window size. Additionally, to address the overfitting issue, we apply a random sampling method to both the state and the reward.

We compare DTF-net with four categorized baselines: trend filtering (TF), change point detection (CPD), anomaly detection (AD), and time series forecasting (TSF) algorithms.

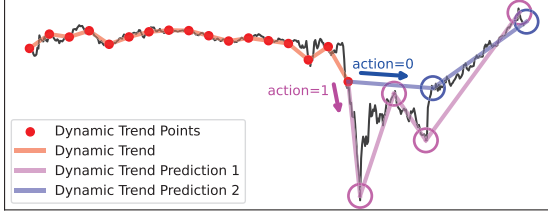


Figure 1: **Dynamic Trend Filtering.** DTF-net extracts dynamic trends from time series data. Dynamic Trend Points (DTPs) are determined based on action predictions, and the dynamic trend is extracted through interpolation. The agent’s action prediction directly influences the variation in trend extraction.

First, traditional TF approaches commonly rely on approximations achieved through optimizing sum-of-squares functions or employing decomposition methods, which often neglect abrupt changes as noise. Second, CPD methods are rooted in probabilistic frameworks, prioritizing the detection of changes in distribution while often disregarding extreme values as outliers. Third, AD methods concentrate heavily on identifying abnormal points, sometimes overlooking the significance of distribution shifts in the data. Lastly, TSF models are categorized into decomposition-based and patching-based models, which also neglect abrupt changes. Contrary to all the aforementioned baselines, DTF-net focuses on point detection to reflect abrupt changes in the trend, enhancing the performance of trend filtering and forecasting. To the best of our knowledge, this is the first approach that employs MDP and RL for trend filtering, aiming to reflect both abrupt changes and smoothness simultaneously.

Therefore, our contributions are as follows:

- We identified the issue of ‘approximateness,’ which leads to constant smoothness in traditional trend filtering, filtering out both abrupt changes and noise.
- We introduce Trend Point Detection formulated as an MDP, aiming to identify essential trend points that should be reflected in the trend, including abrupt changes. Additionally, we propose DTF-net, an RL algorithm that predicts DTPs through agents.
- We employ the forecasting sum-of-squares cost function, inspired by reward function learning based on GP, which allows for the consideration of temporal dependencies when capturing DTPs. A sampling method is applied to prevent the overfitting issue.
- We demonstrate that DTF-net excels at capturing abrupt changes compared to other trend filtering methods and enhances performance in forecasting tasks.

2 Related Work

2.1 Trend Filtering

Traditional trend-filtering algorithms have employed various methods to capture abrupt changes. H-P [Hodrick and Prescott, 1997] and ℓ_1 [Kim *et al.*, 2009] optimize the sum-of-squares function, a widely used cost function for trend filtering. However, they often face challenges in the delayed

detection of abrupt changes due to the use of second-order difference operators for smoothness. To address this issue, the TV-denoising algorithm [Chan *et al.*, 2001] was introduced, relying on first-order differences. Nevertheless, this strategy introduces delays in detecting slow-varying trends while overly focusing on abrupt changes. These methods encounter difficulties in handling heavy-tailed distributions due to the use of the sum-of-squares function [Wen *et al.*, 2019].

Contrary to sum-of-squares function methods, alternative approaches to trend filtering exist. For example, frequency-based methods like Wavelet [Craigmile and Percival, 2002] are designed for non-stationary signals but are susceptible to overfitting. The Empirical Mode Decomposition (EMD) algorithm [Wu *et al.*, 2007] decomposes a time series into a finite set of oscillatory modes, but it generates overly smooth trends. Lastly, the Median filter [Siegel, 1982] is a non-linear filter that selects the middle value from the sorted central neighbors; therefore, outlier values that deviate significantly from the center of the data are excluded.

2.2 Extreme Value Theorem

Abrupt changes in a time series reside in the tail of the data distribution, making them rare events. However, their impact is significant, as they can alter the slope of the time series and affect the consistency of trends. Once an abrupt change occurs, its effects are often permanent until the next one occurs. Therefore, detecting abrupt changes is crucial to minimize false negative rates and capture important information.

Real-world time series data commonly exhibit a long-heavy tail distribution. Formally, the tail distribution is defined as follows:

$$\lim_{T \rightarrow \infty} P\{max(y_1, \dots, y_T) \leq y\} = \lim_{T \rightarrow \infty} F^T(y) = 0, \quad (1)$$

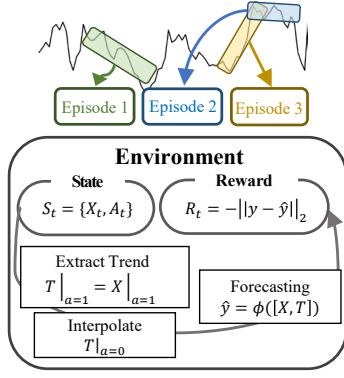
where T random variables $\{y_1, \dots, y_T\}$ are i.i.d. sampled from distribution F_Y [von Bortkiewicz, 1921; Ding *et al.*, 2019]. Furthermore, extreme values within the tail distribution can be modeled using Extreme Value Theory.

Theorem 1 (Extreme Value Theory [Fisher and Tippett, 1928; Ding *et al.*, 2019]). *If the distribution in Equation (1) is not degenerate to 0 under a linear transformation of y , the distribution of the class with the non-degenerate distribution $G(y)$ should be as follows:*

$$G(y) = \begin{cases} \exp(-(1 - \frac{1}{\gamma}y)^\gamma), & \gamma \neq 0, 1 - \frac{1}{\gamma}y \geq 0, \\ \exp(-e^{-y}), & \gamma = 0. \end{cases} \quad (2)$$

Extreme Value Theory (EVT) has demonstrated that extreme values exhibit a limited degree of freedom [Lorenz, 1963]. This implies that the occurrence patterns of extreme values are recursive and can be memorized by a model [Altmann and Kantz, 2005]. Essentially, a model with substantial capacity and temporal invariance can effectively learn abrupt changes, which are categorized as extreme values.

However, extreme values are typically either unlabeled or imbalanced, making them challenging to predict. In classification tasks, previous research [Raj *et al.*, 2016] has highlighted the susceptibility of deep networks to the data im-



(a) DTF-net Environment

	Current Data	Trend for Current (after interpolation)	Future Data	MSE	Reward (= -MSE)
Time Series (scaled)					
Case ①	Action 1 0 1 0 1 0 0 0 1 1 0 0 1 0			0.021	-0.021(mid)
Case ②	Action 1 1 1 0 1 0 0 0 1 0 1 0 1 0			0.032	-0.032(low)
Case ③	Action 1 1 1 0 1 0 0 1 1 1 1 1 0 1			0.008	-0.008(high)

(b) DTF-net Reward

Figure 2: **DTF-net Architecture.** DTF-net has three processes to detect DTPs: 1) The agent predicts actions within a discrete space; 2) With the predicted actions, trends are extracted by interpolating them; 3) The agent is updated through the forecasting sum-of-squares function as a reward; with time series data X and trend T as inputs. For the reward calculation, as demonstrated in (b)-Case 3, when DTF-net successfully identifies abrupt changes, the prediction outcomes significantly improve, resulting in the highest reward.

balance issue. In forecasting tasks, [Ding *et al.*, 2019] provided evidence that minimizing the sum-of-squares loss presupposes a Gaussian distribution, which differs significantly from long-heavy-tail distributions. Motivated by these issues, we define Trend Point Detection as a problem formulation aimed at detecting essential points that should be reflected in the trend rather than smoothed out. This formulation identifies DTPs, which encompass abrupt changes, midpoints of distribution shifts, and other critical points influencing changes in the trend slope, occurring in both short and long intervals. As illustrated in Figure 1, Trend Point Detection is formulated as an MDP and utilizes RL to detect abrupt changes directly through the agent’s action prediction. Note that we train the DNNs as a policy network of an RL agent to learn the pattern of extreme value occurrence, distinct from approximating abrupt changes as output.

2.3 Markov Decision Process and Reinforcement Learning

MDP is a mathematical model for decision-making when an agent interacts with an environment. It relies on the first-order Markov property, indicating that the future state depends solely on the current state. MDP comprises components denoted as $\langle S, A, P, \mathcal{R}, \gamma \rangle$. Here, S denotes the set of environment states, while A represents the set of actions undertaken by the agent at state S . The transition probability, $P = \Pr(S'|S, A)$, signifies the probability of transitioning from the current state S to the next state S' . The reward, $\mathcal{R} = \mathbb{E}[\mathcal{R}(S, A, S')|S, A]$, where $\mathcal{R}(S, A, S')$ represents the immediate reward obtained when transitioning from state S to S' by taking action A . The discount factor $\gamma \in (0, 1]$ governs the trade-off between current and future rewards [Sutton and Barto, 2018]. We can formulate any time series data with an MDP for Trend Point Detection, as detecting points always adheres to the first-order Markov property [Wu and Ortiz, 2021]. These points are determined solely by the current time step and remain unaffected by past observations, sharing properties similar to those of predicting stock trading points.

In RL, actions are predicted through a policy network denoted as $\pi(A|S) = \Pr(A|S)$ for each state, representing the probability of action A at state S . The state-value function $v_\pi(S) = \mathbb{E}_\pi[G|S]$ estimates the expected reward value for a state S under policy π , where $G = \sum_{k=0}^{\infty} \gamma^k \mathcal{R}'_k$ denotes the expected sum of future rewards starting from the next reward \mathcal{R}' . In RL of discrete action spaces, methods like Advantage Actor-Critic (A2C) [Mnih *et al.*, 2016] and Proximal Policy Optimization (PPO) [Schulman *et al.*, 2017] directly train the policy π using the estimated state-value function v . In contrast, Deep Q-Network (DQN) [Mnih *et al.*, 2015] finds the optimal action-value function, denoted as $q_\pi(S, A) = \mathbb{E}_\pi[G|S, A]$. This function represents the expected cumulative reward for taking action A in state S under policy π and is determined through the Bellman equation (Appendix B). DTF-net utilizes RL to extract flexible trends through dynamic action prediction from a deep policy network π , learning within the time series data environment formulated as an MDP of the Trend Point Detection problem.

3 Dynamic Trend Filtering Network

3.1 Trend Point Detection

Environment Definition

Time series data is defined as $\mathbf{T} = \{(\mathbf{X}_1, y_1), (\mathbf{X}_2, y_2), \dots, (\mathbf{X}_N, y_N)\}$, where $\mathbf{X} \in \mathbb{R}^D$ represents the input, $y \in \mathbb{R}^d$ represents the output, and the dataset comprises a total of $N \in \mathbb{Z}^+$ samples. Here, D and d denote the input and output dimensions, respectively, both of which are positive integers.

The Trend Point Detection problem formulation takes input \mathbf{X} representing the environment and outputs DTPs, encompassing abrupt changes, midpoints of distribution shifts, and other critical points influencing trend slope changes occurring at both short and long intervals. The output consists of specific univariate time series $y^{(i)}$ labeled with binary values, where $i \in d$ of target.

- **State** $S = [\mathbf{X}_t, A_t]$: the positional encoded vector set of time series data \mathbf{X} and action A with horizon t .

- **Action** A : a discrete set with ($a = 1$) for detecting DTP and ($a = 0$) for smoothing.
- **Reward** $\mathcal{R}(S, A, S')$: the change in forecasting sum-of-squares function value when action A is taken at state S and results in the transition to the next state S' .
- **Policy** $\pi(A|S)$: the probability distribution of A at S .

The RL algorithm, named DTF-net, employs a policy network π within the defined MDP. It receives the state S as input and outputs the binary labeled target $y^{(i)}$, also denoted as A , learned through the maximization of cumulative rewards \mathcal{R} . DTF-net is designed to extract dynamic trends by interpolating detected essential trend points, referred to as DTPs and represented by the set $\{y^{(i)} = 1\}$ or $\{A|_{a=1}\}$.

Episode and State for DTF-net

Previous studies in RL for time series [Liu *et al.*, 2022a] have generally adopted a sequential approach. In contrast, DTF-net introduces dynamic segmentation with variable lengths comprising one episode through random sampling. The discrete uniform distribution is specifically chosen to ensure that all sub-sequences are considered equally:

$$\begin{aligned} s &\sim \text{unif}\{0, N\}, \\ l &\sim \text{unif}\{h + p, H\}, \end{aligned} \quad (3)$$

where s represents the starting points of the sub-sequence, l denotes the sub-sequence length, h denotes the forecasting look-back horizon, p denotes the forecasting prediction horizon, and H represents the maximum length comprising one episode. With sampling, the length and starting point of the sub-sequence are defined, resulting in a non-sequential and random progression of the episode. This sampling approach mitigates the overfitting issue by allowing the model to use only a portion of the sequence.

Within a single episode, DTF-net cumulatively constructs the state S . To maintain a constant state length within an episode, we employ positional encoding as follows:

$$\begin{aligned} PE_{(pos, 2i)} &= \sin(pos/10000^{2i/d_{model}}), \\ PE_{(pos, 2i+1)} &= \cos(pos/10000^{2i/d_{model}}). \end{aligned}$$

The cumulative state progression is achieved by gradually expanding the state representation S_t as the step unfolds as follows,

$$S_t = PE(\{\mathbf{X}_{s:s+t}, A_{0:t}\}), \text{ where } t < l. \quad (4)$$

Through cumulative state construction, the agent can learn sequential information in the time series (Appendix D.1).

3.2 Reward Function of DTF-net

GP and Reward Function Learning

Traditional trend filtering methods utilize the sum-of-squares function, also known as the Mean Squared Error (MSE), to approximate abrupt changes when extracting trends. However, [Ding *et al.*, 2019] provided evidence that minimizing the sum-of-squares function assumes that the model output distribution determined using the MSE cost function denoted

Algorithm 1 Reward Procedure of DTF-net

```

procedure REWARD( $S_t$ )
   $\mathbf{X}' = \mathbf{X}_{t-(h+p):t}$ ,  $A' = A_{t-(h+p):t}$ 
   $\mathcal{T} \leftarrow 0$ 
   $\mathcal{T}|_{a=1} \leftarrow \mathbf{X}'_{0:h}|_{a=1}$ 
  while  $n \leq h$  do
    //  $n$  for time-axis and  $\mathbf{x} \in \mathbf{X}'$ 
     $\mathcal{T}_n \leftarrow \mathbf{x}_n = \mathbf{x}_{n-1} + \frac{\mathbf{x}_{n+1} - \mathbf{x}_{n-1}}{2}$ 
     $n \leftarrow n + 1$ 
  end while
   $\hat{y} \leftarrow \phi([\mathbf{X}'_{0:h}, \mathcal{T}])$ 
   $r \leftarrow \frac{1}{p} \sum_{i=1}^p (y_i - \hat{y}_i)^2$ 
  return  $-r$ 
end procedure

```

as $\hat{P}(Y)$, follows a Gaussian distribution with variance τ , grounded in Bregman's theory [Banerjee *et al.*, 2005].

$$\begin{aligned} \hat{P}(Y) &= \min \sum_{t=1}^T \|y_t - o_t\|^2, \\ &= \max_{\theta} \prod_{t=1}^T P(y_t | x_t, \theta), \\ &= \frac{1}{N} \sum_{t=1}^T \mathcal{N}(y_t, \hat{\tau}^2). \end{aligned} \quad (5)$$

where $o \in Y$ represents the output from a model parameterized by θ . This also suggests that model θ operates in a manner similar to a Kernel Density Estimator (KDE) employing a Gaussian kernel [Rosenblatt, 1956].

Contrary to approximations, DTF-net utilizes a policy network π to predict DTPs, including abrupt changes. However, defining a reward function in general time series data is challenging but is the most crucial task in RL training for optimizing the policy network. To tackle this challenge, DTF-net draws inspiration from previous works, which employ the Gaussian Process (GP) for reward function learning [Kuss and Rasmussen, 2003; Biyik *et al.*, 2020].

Formally, GP [Williams and Rasmussen, 1995] assumes noisy targets $y_i = f(x_i) + \epsilon_i$ that are jointly Gaussian with a covariance function k :

$$P(y|x) \sim \mathcal{N}(0, \mathbf{K}), \text{ where } \mathbf{K}_{pq} = k(x_p, x_q). \quad (6)$$

With a Gaussian covariance function,

$$k(x_p, x_q | \theta) = v^2 \exp(-(x_p - x_q)^\top \Lambda^{-1} (x_p - x_q) / 2) + \delta_{pq} \sigma_n^2,$$

where diagonal matrix Λ , v , and σ are hyperparameters in θ , the predictive distribution for input x^* follows Gaussian:

$$\begin{aligned} P(o_t^* | x^*, x, y, \theta) &\sim \mathcal{N}(k(x^*, x) \mathbf{K}^{-1} y, \\ &\quad k(x^*, x^*) - k(x^*, x) \mathbf{K}^{-1} k(x, x^*)). \end{aligned} \quad (7)$$

The GP model inherently learns a full distribution of time series data, enabling RL to effectively optimize the policy network (Appendix B). Leveraging these insights, DTF-net's reward function is defined as the sum-of-squares function from

Trend Filtering		Linear Signal+Noise (0.2)			
		1) full-sequence		2) abrupt-sequence	
		MSE	MAE	MSE	MAE
CPD	ADAGA [Caldarelli <i>et al.</i> , 2022]	4.3434	1.4428	7.0120	1.8668
	RED-SDS [Ansari <i>et al.</i> , 2021]	1.0036	0.6782	1.6660	0.9365
AD	TimesNet [Wu <i>et al.</i> , 2023]	3.0841	1.4204	3.3304	1.4364
	AnomalyTransformer [Xu <i>et al.</i> , 2022]	7.7506	2.1817	10.1336	2.7242
	DCdetector [Yang <i>et al.</i> , 2023]	<u>0.0094</u>	<u>0.0255</u>	3.6300	1.3721
TF	EMD [Wu <i>et al.</i> , 2007]	5.3096	1.7401	6.4410	1.8431
	Median [Siegel, 1982]	4.4766	1.5525	5.6859	1.8204
	H-P [Hodrick and Prescott, 1997]	0.2253	0.3311	0.3238	0.3934
	Wavelet [Craigmile and Percival, 2002]	$1e-30$	$6e-16$	$2e-30$	$8e-16$
	ℓ_1 ($\lambda=0.1$) [Kim <i>et al.</i> , 2009]	<u>0.0461</u>	<u>0.1703</u>	<u>0.0500</u>	<u>0.1807</u>
	ℓ_1 ($\lambda = 5e-4$)	0.0004	0.0175	0.0004	0.0174
	DTF-net (ours)	0.0289	0.0826	0.0286	0.0855

Table 1: **Comparison with advanced CPD, AD, and TF methods in synthetic data.** We conduct trend filtering analysis on synthetic data, evaluating it against the ground truth of a linear signal with added noise. We consider two cases: one with the full sequence and the other with a 30-window interval sub-sequence containing abrupt changes. The evaluation metrics are Mean Squared Error (MSE) and Mean Absolute Error (MAE), where lower values indicate better performance. The best performance is **bolded**, and the second-best performance is underlined. For the special case of DCdetector, the performance is denoted in *italic*.

Time Series Forecasting (TSF). This choice leads to more efficiency in calculating rewards compared to GP while achieving reward function learning within the Gaussian distribution. To incorporate captured abrupt changes into the forecasting model, DTPs are included as an additional input. As shown in Figure 2, when the forecasting model predicts upward or downward trends instead of smoothing them out, the agent receives a higher reward. Thus, DTF-net learns temporal dependencies when capturing DTPs.

Forecasting Reward Function of DTF-net

As shown in Algorithm 1, the reward process involves time series data $\mathbf{X}_{t-(h+p):t}$ and action $A_{t-(h+p):t}$ in state S_t at time step t , both having a sequence length denoted as $(h+p)$, where h denotes the past horizon and p denotes the forecasting horizon (under the condition $t - (h+p) > 0$). The trend \mathcal{T} initiates with \mathbf{X} values assigned only under the condition of action $A|_{a=1}$, and linear interpolation is applied for the remaining values. Subsequently, forecasting is conducted with a prediction length p defined by a hyperparameter. The reward is computed as the negative sum-of-squares loss between the predicted \hat{y} and the ground truth y .

DTF-net uses a penalty reward as a negative value from the Mean Squared Error (MSE) function, and there is a possibility of an overfitting issue. Therefore, DTF-net utilizes random sampling from a discrete uniform distribution, providing better control over model updates.

$$k \sim \text{unif}\{s, s+l\},$$

$$R = \begin{cases} \text{REWARD}(E_t) & \text{if } t = k, \\ 0 & \text{if } t \neq k. \end{cases} \quad (8)$$

We empirically demonstrate that irregularly applying penalties through sampling can prevent overfitting rather than penalizing at every step in Section 4.2 (Appendix D.2).

In summary, DTF-net is designed to extract dynamic trends \mathcal{T} by interpolating detected DTPs. A simple ML time series predictor ϕ is integrated into DTF-net to calculate the reward, with the input of $[\mathbf{X}, \mathcal{T}]$. As shown in Figure 2, including

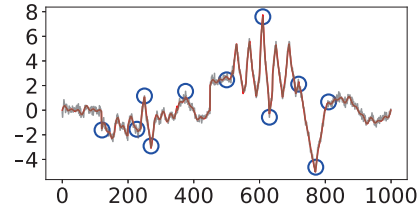


Figure 3: **Synthetic Data.**

the detected abrupt changes as an additional input to the forecasting model ensures that the forecasting output reflects both upward and downward trends, maximizing the reward.

4 Experiment

4.1 Trend Filtering Analysis

Experimental Settings

Analyzing trend filtering methods quantitatively poses two challenges: 1) defining a ground truth for the trend is challenging, and 2) labeling abrupt changes is challenging. To address these, as shown in Figure 3, we generate a synthetic trend signal with 1,000 time points. This synthetic dataset contains 11 abrupt changes, including 1) a sudden drop to negative values around -2 and -5 at time points 100 and 800, respectively; 2) a mean shift from 0 to 4 with high variance occurring between time points 500 and 700; and 3) a sine wave starting from time point 800 to 1000, completing one cycle. We add Gaussian noise with a standard deviation of 0.2 to simulate real-world conditions.

To evaluate the trend filtering results, we set up the experiment as follows. We employ Mean Squared Error (MSE) and Mean Absolute Error (MAE) metrics to measure the proximity to the original data, which is a key aspect of trend filtering. For the ground truth, we use a linear signal with added noise to assess DTF-net’s robustness to noisy data. In cases with added noise, we assume that filtering out at least 10%

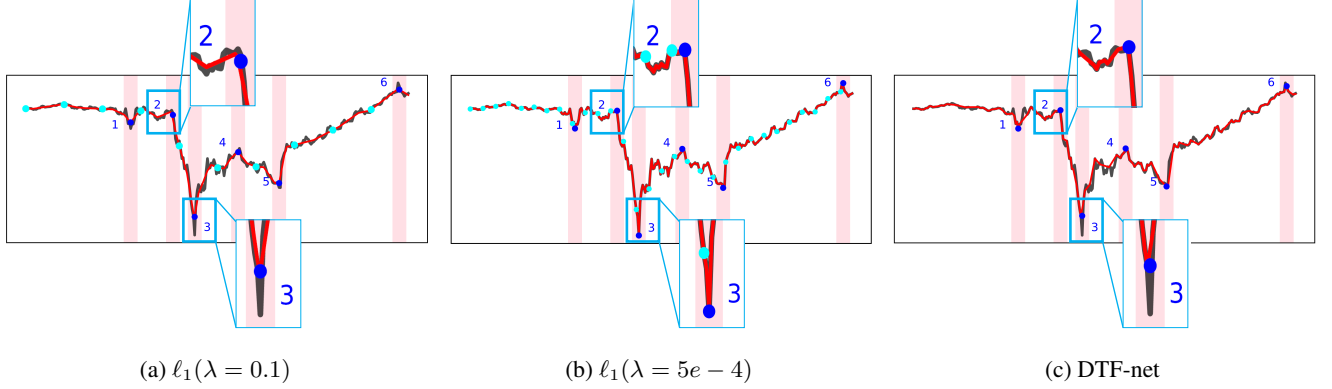


Figure 4: **Qualitative comparison with ℓ_1 and DTF-net.** The figure illustrates the trends obtained from the ℓ_1 and DTF-net using the Nasdaq intraday dataset. The red line denotes the output of each trend filtering method, with red vertical boxes indicating arbitrarily set abrupt changes. The blue dots denote the captured abrupt changes, while the sky-blue dots highlight the constant smoothness from ℓ_1 . Notably, DTF-net has the capability to apply varying levels of smoothness to individual sub-sequences.

Methods		DTF-Linear (ours)		$\ell_1(\lambda = 0.1)$ -Linear		PatchTST/42		NLinear		DLinear		FEDformer-f		FEDformer-w		Autoformer	
Metric		MSE	MAE	MSE	MAE	MSE	MAE	MSE	MAE	MSE	MAE	MSE	MAE	MSE	MAE	MSE	MAE
Exchange	24	0.0250	0.1198	0.0266	0.1248	0.0387	0.1513	0.0275	<u>0.1264</u>	0.0290	0.1284	0.0381	0.1545	0.0387	0.1564	0.0687	0.2041
	48	0.0487	0.1658	0.0505	0.1708	0.0624	0.1873	<u>0.0505</u>	<u>0.1705</u>	0.0585	0.1907	0.0548	0.1818	0.1068	0.2528	0.1095	0.2485
	96	0.0980	0.2349	0.1007	0.2440	0.1833	0.3436	<u>0.0990</u>	<u>0.2361</u>	0.1063	0.2530	0.1440	0.2980	0.1386	0.2894	0.1834	0.3306
	192	0.1983	0.3583	0.2045	0.3518	0.2550	0.3987	0.2030	<u>0.3400</u>	<u>0.1959</u>	0.3554	0.2790	0.4163	0.2841	0.4217	0.3465	0.4510
	336	0.3160	0.4561	0.3337	0.4666	0.5161	0.5442	0.4174	0.4857	<u>0.3276</u>	<u>0.4627</u>	0.4466	0.5130	0.5685	0.5890	0.4488	0.5291
	720	0.7933	0.6874	0.9515	0.7636	1.1143	0.8063	1.0420	0.7807	<u>0.9071</u>	<u>0.7415</u>	1.2122	0.8492	1.2912	0.8876	1.2463	0.8694
ETTh1	24	0.0253	0.1205	<u>0.0234</u>	<u>0.1140</u>	0.0266	0.1238	0.0266	0.1240	0.0273	0.1262	0.0358	0.1450	0.0381	0.1524	0.0694	0.2042
	48	0.0375	0.1479	<u>0.0366</u>	<u>0.1442</u>	0.0393	0.1506	<u>0.0388</u>	<u>0.1503</u>	0.0404	0.1523	0.0547	0.1778	0.0602	0.1921	0.0797	0.2205
	96	0.0519	0.1740	0.0521	0.1744	0.0550	0.1790	<u>0.0519</u>	<u>0.1745</u>	0.0551	0.1815	0.0786	0.2126	0.0919	0.2348	0.0857	0.2292
	192	0.0676	0.2013	0.0693	0.2034	0.0705	0.2050	<u>0.0694</u>	<u>0.2046</u>	0.0730	0.2076	0.0933	0.2344	0.1000	0.2464	0.0993	0.2428
	336	0.0803	0.2247	<u>0.0796</u>	<u>0.2238</u>	0.0814	0.2260	0.0826	0.2280	0.0948	0.2414	0.1117	0.2597	0.1418	0.2958	0.1287	0.2792
	720	0.0776	0.2224	0.0789	0.2244	0.0869	0.2329	<u>0.0814</u>	<u>0.2273</u>	0.1800	0.3494	0.1310	0.2858	0.1224	0.2766	0.1378	0.2939
Illness	24	0.5881	0.5358	0.6119	<u>0.5299</u>	<u>0.6228</u>	<u>0.5305</u>	0.6325	0.5639	0.7831	0.7462	0.6969	0.6256	0.7100	0.6352	0.7432	0.6704
	48	0.6858	0.6359	0.6925	0.6322	0.7109	0.6642	<u>0.6892</u>	<u>0.6453</u>	0.8217	0.7750	0.7099	0.6935	0.6961	0.6972	0.7855	0.7370
	60	0.6640	0.6423	0.6666	<u>0.6324</u>	0.6465	0.6381	0.6730	<u>0.6347</u>	0.9195	0.8361	0.8309	0.7653	0.8192	0.7641	0.8945	0.8055

Table 2: **Evaluating DTF-net in TSF task.** We conduct TSF experiments using three non-stationary datasets: Exchange Rate, ETTh1, and Illness. We evaluate performance using MSE and MAE, where lower values indicate better performance. In the following results, the best-performing models using DTF-net are highlighted in **bold**, and models using ℓ_1 trend filtering are highlighted in *italic*. Additionally, for comparison, the best-performing models using only original data are underlined.

of noise is necessary to confirm smoothness. We divide the proximity evaluation into two categories: full-sequence and sub-sequence. In the sub-sequence evaluation, a 30-window interval is set around labeled abrupt changes to assess temporal dependencies are well captured.

Performance Analysis

Table 1 emphasizes DTF-net’s superior performance compared to CPD and AD algorithms. CPD algorithms are designed to identify shifts in data distribution and tend to capture the midpoint of these changes, treating extreme values as outliers. On the other hand, AD algorithms focus exclusively on pinpointing anomalous data points, often overlooking the midpoint of changes. For instance, DCdetector is particularly adept at identifying abnormal values, demonstrating superior performance across entire data sequences. However, its effectiveness diminishes when dealing with abrupt sub-sequences. This shortfall stems from its focus solely on detecting abnormal points and short intervals surrounding abrupt changes. Consequently, while it maintains commendable performance on full sequences, it falls short in accurately filtering trends

within abrupt sub-sequences. In essence, the differing objectives of CPD and AD algorithms make them less suitable for trend-filtering (Figure 7 in Appendix A).

In comparison with other trend filtering methods, DTF-net outperforms all methods except those prone to overfitting. Decomposition-based methods like EMD and Median generate excessively smoothed trends. The frequency-based method, Wavelet, tends to overfit to noise. The ℓ_1 method shows sensitivity to hyperparameter λ , as evident by $\lambda = 5e - 4$ causing overfitting to noise. Therefore, DTF-net excels in capturing abrupt changes while reflecting temporal dependencies within noisy and complex time series data.

Nasdaq Dataset

To demonstrate the proficiency of DTF-net on complex real-world datasets, we perform additional analysis on the Nasdaq intraday dataset from July 30th to August 1st, 2019, characterized by rapid changes. Here, we arbitrarily set 6 abrupt changes and qualitatively analyze the results. As shown in Figure 4, it is evident that the ℓ_1 trend filtering algorithm extracts trends that either underfit or overfit depending on the

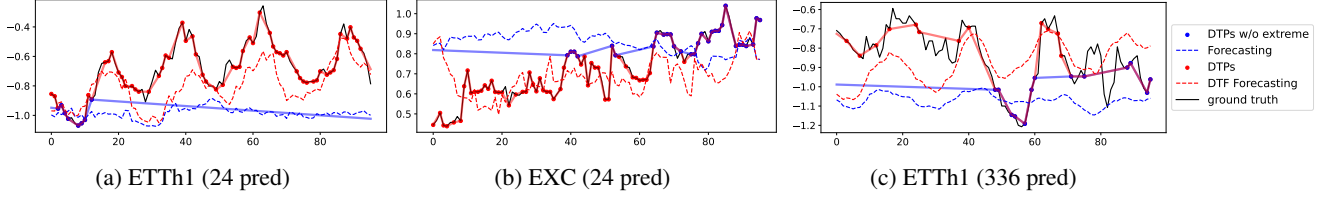


Figure 5: **Qualitative analysis of the impact of abrupt changes on TSF.** We conduct forecasting experiments to evaluate the influence of trends incorporating extreme values with long-heavy tails on two datasets, ETTh1 and Exchange rate (EXC). The figure illustrates that including abrupt changes (red) in forecasting plays a crucial role without undergoing smoothing (blue). It is evident that the results appear smoother when extreme values are excluded (depicted by the blue line) in both short-term (24 pred) and long-term (336 pred) forecasting.

parameter λ due to constant smoothness. For point 3, in detail, ℓ_1 with ($\lambda = 0.1$) filtered out noise, while ($\lambda = 5e - 4$) captured it as abrupt changes. In contrast, DTF-net accurately captures five abrupt changes and concurrently performs noise filtering for point 3. This accomplishment is attributed to the dynamic nature of trend extraction from DTF-net.

4.2 Trend Filtering in Time Series Forecasting

Experimental Settings

We analyze how DTF-net effectively captures abrupt changes and extend our evaluation to include a real-world dataset for a common time series task. Time Series Forecasting (TSF) models are expected to predict potential incidents associated with extreme values, providing valuable insights for critical decision-making [Van den Berg *et al.*, 2008]. To assess the practicality of DTF-net in real-world scenarios, we apply it to TSF, incorporating the extracted trend as an additional input feature. Formally, the forecasting model receives input as $\mathbf{X}' = [\mathbf{X}, \mathbf{P}] \in \mathbb{R}^{D+1}$, where \mathbf{P} represents the trend from DTF-net. Under the same conditions, we compare this model to those using ℓ_1 as additional inputs and only the original sequence \mathbf{X} as inputs. We employ DTF-net with the TSF models NLinear and DLinear [Zeng *et al.*, 2023], which are considered state-of-the-art yet simplest in the field of TSF. The experiment focuses on the univariate forecasting case to assess trend filtering effectiveness (Appendix C). Note that DTF-net is not directly linked with TSF models; instead, the extracted trend from DTF-net is provided as additional input.

Performance Analysis

We choose three non-stationary datasets from the TSF benchmark dataset: Exchange Rate, ETTh1, and Illness (Appendix C.1). Table 2 indicates that DTF-net outperforms in most cases. Among the three datasets, the exchange rate dataset is the most intricate, exhibiting the least seasonality and the highest level of noise. Given the absence of periodicity in financial data, ℓ_1 trend filtering encounters difficulties in extracting clear trends. However, DTF-net demonstrates robustness when dealing with non-stationary time series data.

However, models employing ℓ_1 trend filtering have advantages when dealing with more stationary data that exhibits a recursive pattern. The piece-wise linearity assumption of ℓ_1 is particularly pronounced in short-term predictions within ETTh1, as it is the least noisy and most stationary dataset among the three. As shown in Table 2, ℓ_1 achieves

the best results for 24- and 48-hour forecasting windows in ETTh1. While DTF-net also outperforms the single forecasting model, the linearity characteristic of ℓ_1 is better suited for short-term predictions within ETTh1. In contrast, for long-term predictions, we demonstrate that DTF-net performs the best. In the case of Illness with a small dataset size, DTF-net also performs well without overfitting.

Ablation Study

How to prevent RL overfitting? To mitigate the risk of overfitting in RL-based trend filtering, we introduce a reward sampling method. As shown in Figure 9, we observe that reward sampling prevents overfitting, achieving optimal performance with a reward sampling (Appendix B.4).

Empirical analysis on extreme value DNNs often generate smooth and averaged predictions as they typically optimize forecasting performance through empirical risk minimization. However, by incorporating accurately captured abrupt changes as additional information into the model, predictions are enhanced while representing both upward and downward signals instead of providing solely smooth estimates. To qualitatively assess the impact of abrupt changes on forecasting tasks, we compare two different trends: the original trends from DTF-net (red) and a version where 10% of extreme values are excluded (blue). As shown in Figure 5, this comparison demonstrates how incorporating abrupt changes can enrich forecasting by providing more detailed and accurate predictions.

5 Conclusion

We propose DTF-net, a novel RL-based trend filtering method directly identifying trend points. Traditional trend filtering methods struggle to capture abrupt changes due to their inherent approximations. To address this, we formalize the Trend Point Detection problem as an MDP and utilize RL within a discrete action space. The reward function is defined as the sum-of-squares loss from forecasting tasks inspired by reward function learning within the Gaussian distribution, allowing for the capturing of temporal dependencies around DTFs. DTF-net also tackles overfitting issues through random sampling. Compared to other trend filtering methods, DTF-net excels in identifying abrupt changes. In forecasting tasks, DTF-net enhances predictive performance without compromising the prediction output to be smooth.

Acknowledgments

This work was partly supported by Institute of Information & Communications Technology Planning & Evaluation (IITP) grant funded by the Korea government (MSIT) (No. 2022-0-00984, Development of Artificial Intelligence Technology for Personalized Plug-and-Play Explanation and Verification of Explanation; No. 2022-0-00184, Development and Study of AI Technologies to Inexpensively Conform to Evolving Policy on Ethics; No. 2021-0-02068, Artificial Intelligence Graduate School Program (KAIST)).

References

- [Adams and MacKay, 2007] Ryan Prescott Adams and David JC MacKay. Bayesian online changepoint detection. *arXiv preprint arXiv:0710.3742*, 2007.
- [Altmann and Kantz, 2005] Eduardo G Altmann and Holger Kantz. Recurrence time analysis, long-term correlations, and extreme events. *Physical Review E*, 71(5):056106, 2005.
- [Ansari et al., 2021] Abdul Fatir Ansari, Konstantinos Benidis, Richard Kurle, Ali Caner Turkmen, Harold Soh, Alexander J Smola, Bernie Wang, and Tim Januschowski. Deep explicit duration switching models for time series. In *Proceedings of Advances in Neural Information Processing Systems (NeurIPS'21)*, 2021.
- [Banerjee and Gelfand, 2003] Sudipto Banerjee and AE Gelfand. On smoothness properties of spatial processes. *Journal of Multivariate Analysis*, 84(1):85–100, 2003.
- [Banerjee et al., 2005] Arindam Banerjee, Srujana Merugu, Inderjit S Dhillon, Joydeep Ghosh, and John Lafferty. Clustering with bregman divergences. *Journal of Machine Learning Research*, 6(10), 2005.
- [Biyik et al., 2020] Erdem Biyik, Nicolas Huynh, Mykel J. Kochenderfer, and Dorsa Sadigh. Active preference-based gaussian process regression for reward learning. In *Proceedings of Robotics: Science and Systems (RSS'20)*, 2020.
- [Caldarelli et al., 2022] Edoardo Caldarelli, Philippe Wenk, Stefan Bauer, and Andreas Krause. Adaptive Gaussian process change point detection. In *Proceedings of International Conference on Machine Learning (ICML'22)*, 2022.
- [Chan et al., 2001] Tony F Chan, Stanley Osher, and Jianhong Shen. The digital tv filter and nonlinear denoising. *IEEE Transactions on Image processing*, 10(2):231–241, 2001.
- [Chow, 1960] Gregory C Chow. Tests of equality between sets of coefficients in two linear regressions. *Econometrica: Journal of the Econometric Society*, pages 591–605, 1960.
- [Craigmile and Percival, 2002] Peter F Craigmile and Donald B Percival. Wavelet-based trend detection and estimation. *Entry in the Encyclopedia of Environmetrics*. Chichester, UK: John Wiley & Sons, pages 2334–2338, 2002.
- [Dickey and Fuller, 1979] David A Dickey and Wayne A Fuller. Distribution of the estimators for autoregressive time series with a unit root. *Journal of the American Statistical Association*, 74(366a):427–431, 1979.
- [Ding et al., 2019] Daizong Ding, Mi Zhang, Xudong Pan, Min Yang, and Xiangnan He. Modeling extreme events in time series prediction. In *Proceedings of ACM SIGKDD International Conference on Knowledge Discovery and Data Mining (KDD'19)*, 2019.
- [Fisher and Tippett, 1928] Ronald Aylmer Fisher and Leonard Henry Caleb Tippett. Limiting forms of the frequency distribution of the largest or smallest member of a sample. In *Mathematical Proceedings of the Cambridge Philosophical Society*, 1928.
- [Geyer, 1992] Charles J. Geyer. Practical Markov Chain Monte Carlo. *Statistical Science*, 7(4):473 – 483, 1992.
- [Gong and Huang, 2012] Rongsheng Gong and Samuel H. Huang. A kolmogorov-smirnov statistic based segmentation approach to learning from imbalanced datasets: With application in property refinane prediction. *Expert Syst. Appl.*, 39(6):6192–6200, may 2012.
- [Hallac et al., 2017] David Hallac, Sagar Vare, Stephen Boyd, and Jure Leskovec. Toeplitz inverse covariance-based clustering of multivariate time series data. In *Proceedings of ACM SIGKDD International Conference on Knowledge Discovery and Data Mining (KDD'17)*, 2017.
- [Han et al., 2019] Jiyeon Han, Kywoon Lee, Anh Tong, and Jaesik Choi. Confirmatory bayesian online change point detection in the covariance structure of gaussian processes. In *Proceedings of International Joint Conference on Artificial Intelligence (IJCAI'19)*, 2019.
- [Hodrick and Prescott, 1997] Robert J Hodrick and Edward C Prescott. Postwar us business cycles: an empirical investigation. *Journal of Money, credit, and Banking*, pages 1–16, 1997.
- [Kim et al., 2009] Seung-Jean Kim, Kwangmoo Koh, Stephen Boyd, and Dmitry Gorinevsky. ℓ_1 trend filtering. *SIAM review*, 51(2):339–360, 2009.
- [Kuss and Rasmussen, 2003] Malte Kuss and Carl Rasmussen. Gaussian processes in reinforcement learning. In *Proceedings of Advances in Neural Information Processing Systems (NeurIPS'03)*, 2003.
- [Leser, 1961] Conrad Emanuel Victor Leser. A simple method of trend construction. *Journal of the Royal Statistical Society: Series B (Methodological)*, 23(1):91–107, 1961.
- [Liu et al., 2022a] Xiao-Yang Liu, Ziyi Xia, Jingyang Rui, Jiechao Gao, Hongyang Yang, Ming Zhu, Christina Dan Wang, Zhaoran Wang, and Jian Guo. Finrl-meta: Market environments and benchmarks for data-driven financial reinforcement learning. In *Proceedings of Advances in Neural Information Processing Systems (NeurIPS'22)*, 2022.
- [Liu et al., 2022b] Yong Liu, Haixu Wu, Jianmin Wang, and Mingsheng Long. Non-stationary transformers: Exploring the stationarity in time series forecasting. In *Proceed-*

- ings of *Advances in Neural Information Processing Systems (NeurIPS'22)*, 2022.
- [Lorenz, 1963] Edward N Lorenz. Deterministic nonperiodic flow. *Journal of Atmospheric Sciences*, 20(2):130–141, 1963.
- [Mnih *et al.*, 2015] Volodymyr Mnih, Koray Kavukcuoglu, David Silver, Andrei A Rusu, Joel Veness, Marc G Bellemare, Alex Graves, Martin Riedmiller, Andreas K Fidjeland, Georg Ostrovski, et al. Human-level control through deep reinforcement learning. *Nature*, 518(7540):529–533, 2015.
- [Mnih *et al.*, 2016] Volodymyr Mnih, Adria Puigdomenech Badia, Mehdi Mirza, Alex Graves, Timothy Lillicrap, Tim Harley, David Silver, and Koray Kavukcuoglu. Asynchronous methods for deep reinforcement learning. In *Proceedings of International Conference on Machine Learning (ICML'16)*, 2016.
- [Nie *et al.*, 2023] Yuqi Nie, Nam H. Nguyen, Phanwadee Sinthong, and Jayant Kalagnanam. A time series is worth 64 words: Long-term forecasting with transformers. In *Proceedings of International Conference on Learning Representations (ICLR'23)*, 2023.
- [Park *et al.*, 2020] Youngjin Park, Deokjun Eom, Byoungki Seo, and Jaesik Choi. Improved predictive deep temporal neural networks with trend filtering. In *Proceedings of ACM International Conference on AI in Finance (ICAIF'20)*, 2020.
- [Ploberger and Krämer, 1992] Werner Ploberger and Walter Krämer. The cusum test with ols residuals. *Econometrica: Journal of the Econometric Society*, pages 271–285, 1992.
- [Raj *et al.*, 2016] Vidwath Raj, Sven Magg, and Stefan Wermter. Towards effective classification of imbalanced data with convolutional neural networks. *Artificial Neural Networks in Pattern Recognition*, pages 150–162, 2016.
- [Rosenblatt, 1956] Murray Rosenblatt. Remarks on some nonparametric estimates of a density function. *The Annals of Mathematical Statistics*, pages 832–837, 1956.
- [Schulman *et al.*, 2017] John Schulman, Filip Wolski, Prafulla Dhariwal, Alec Radford, and Oleg Klimov. Proximal policy optimization algorithms. *arXiv preprint arXiv:1707.06347*, 2017.
- [Siegel, 1982] Andrew F Siegel. Robust regression using repeated medians. *Biometrika*, 69(1):242–244, 1982.
- [Sutton and Barto, 2018] Richard S Sutton and Andrew G Barto. *Reinforcement learning: An introduction*. MIT press, 2018.
- [Van den Berg *et al.*, 2008] Jeroen Van den Berg, Bertrand Candelson, and Jean-Pierre Urbain. A cautious note on the use of panel models to predict financial crises. *Economics Letters*, 101(1):80–83, 2008.
- [von Bortkiewicz, 1921] Ladislaus von Bortkiewicz. *Variationsbreite und mittlerer Fehler*. Berliner Mathematische Gesellschaft, 1921.
- [Wen *et al.*, 2019] Qingsong Wen, Jingkun Gao, Xiaomin Song, Liang Sun, and Jian Tan. Robusttrend: A huber loss with a combined first and second order difference regularization for time series trend filtering. In *Proceedings of International Joint Conference on Artificial Intelligence (IJCAI'19)*, 2019.
- [Williams and Rasmussen, 1995] Christopher Williams and Carl Rasmussen. Gaussian processes for regression. In *Proceedings of Advances in Neural Information Processing Systems (NeurIPS'95)*, 1995.
- [Wu and Ortiz, 2021] Tong Wu and Jorge Ortiz. Rlad: Time series anomaly detection through reinforcement learning and active learning. *ArXiv*, abs/2104.00543, 2021.
- [Wu *et al.*, 2007] Zhaohua Wu, Norden E Huang, Steven R Long, and Chung-Kang Peng. On the trend, detrending, and variability of nonlinear and nonstationary time series. *National Academy of Sciences*, 104(38):14889–14894, 2007.
- [Wu *et al.*, 2021] Haixu Wu, Jiehui Xu, Jianmin Wang, and Mingsheng Long. Autoformer: Decomposition transformers with auto-correlation for long-term series forecasting. In *Proceedings of Advances in Neural Information Processing Systems (NeurIPS'21)*, 2021.
- [Wu *et al.*, 2023] Haixu Wu, Tengge Hu, Yong Liu, Hang Zhou, Jianmin Wang, and Mingsheng Long. Timesnet: Temporal 2d-variation modeling for general time series analysis. In *Proceedings of International Conference on Learning Representations (ICLR'23)*, 2023.
- [Xu *et al.*, 2022] Jiehui Xu, Haixu Wu, Jianmin Wang, and Mingsheng Long. Anomaly transformer: Time series anomaly detection with association discrepancy. In *Proceedings of International Conference on Learning Representations (ICLR'22)*, 2022.
- [Yang *et al.*, 2023] Yiyuan Yang, Chaoli Zhang, Tian Zhou, Qingsong Wen, and Liang Sun. Dcdetector: Dual attention contrastive representation learning for time series anomaly detection. In *Proceedings of ACM SIGKDD International Conference on Knowledge Discovery and Data Mining (KDD'23)*, 2023.
- [Zeng *et al.*, 2023] Ailing Zeng, Muxi Chen, Lei Zhang, and Qiang Xu. Are transformers effective for time series forecasting? In *Proceedings of the AAAI Conference on Artificial Intelligence (AAAI'23)*, 2023.
- [Zhou *et al.*, 2021] Haoyi Zhou, Shanghang Zhang, Jieqi Peng, Shuai Zhang, Jianxin Li, Hui Xiong, and Wancai Zhang. Informer: Beyond efficient transformer for long sequence time-series forecasting. In *Proceedings of the AAAI Conference on Artificial Intelligence (AAAI'20)*, 2021.
- [Zhou *et al.*, 2022] Tian Zhou, Ziqing Ma, Qingsong Wen, Xue Wang, Liang Sun, and Rong Jin. Fedformer: Frequency enhanced decomposed transformer for long-term series forecasting. In *Proceedings of International Conference on Machine Learning (ICML'22)*, 2022.

A Extended Related Work

Abrupt changes represent a shift in the slope of the trend and are categorized as extreme values. Focusing on this characteristic, we delve into algorithms specifically designed to identify points that share similar concepts with abrupt changes, such as structural breakpoints, change points, and anomaly points. Additionally, we discuss why these algorithms may not be suitable for trend-filtering tasks.

A.1 Structural Break Point and Change Point Detection

Statistical Test

A Structural Break Point (SBP) signifies an unexpected change in time series data. Various statistical algorithms can validate identified SBPs, including Chow [Chow, 1960], Augmented Dickey-Fuller (ADF) [Dickey and Fuller, 1979], and CUSUM [Ploberger and Krämer, 1992]. These methods confirm whether the detected points are structural breaks, relying on statistical tests using the F-value. In practical applications, algorithms should not only validate detected SBPs but also predict them in an online manner. The online approach involves predicting based on past to current state as data arrives incrementally over time, while the offline approach is prediction based on the entire dataset at once. Figure 6-(a) illustrates the results of detected SBPs in an offline manner based on the maximum F-value, comparing two subsequences while moving time points one by one. Each algorithm detects SBPs based on its own rule, resulting in irregular breakpoints that are challenging to adapt to the trend. This offline approach is highly sensitive to the input length and requires the heuristic definition of an additional threshold for breakpoint detection.

Change Point Detection

A change point denotes a specific time point or position within a time series where a significant shift or change occurs in the statistical properties of the data. Change Point Detection (CPD) algorithms specialize in identifying these shifts in distribution. One notable CPD approach is Bayesian Online Change Point Detection (BOCPD) [Adams and MacKay, 2007]. This method detects points by maintaining a probability distribution over possible change points and updating this distribution as new data points are observed. However, BOCPD faces practical limitations due to its assumption of independence and the presence of temporal correlations between samples. Additionally, sensitivity to hyperparameters is a drawback of BOCPD [Han *et al.*, 2019]. Essentially, the probabilistic approach tends to overlook extreme values as outliers, leading to the detection of only the mean shift.

The Kolmogorov-Smirnov (KS) test-based segmentation [Gong and Huang, 2012] assesses whether two data samples originate from the same underlying cumulative distribution. However, the KS algorithm is designed for offline detection, implying that it evaluates the entire time series at once. RED-SDS [Ansari *et al.*, 2021] is a supervised learning method for segmentation, utilizing switching behavior to understand the underlying dynamical system in time series. However, as a supervised approach, RED-SDS requires a preceding labeling process to accurately train the model on correct change

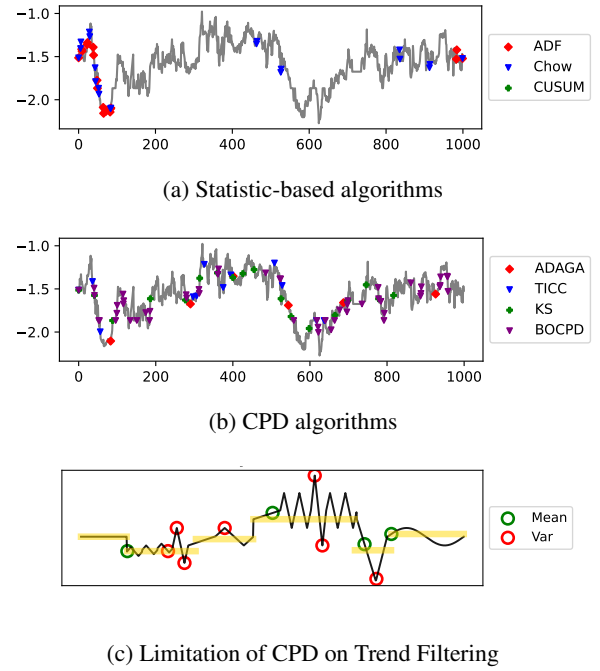


Figure 6: **Limitation of SBP and CPD algorithms in trend filtering.** Figures (a) and (b) illustrate how statistical-based and CPD algorithms detect abrupt changes based on their own criteria in a real-world dataset, ETTh1. The detected points appear irregular, making them challenging to adapt to the trends. In general, Figure (c) illustrates the difficulties CPD algorithms face when identifying points where there is no mean shift and only variance perturbation occurs, as highlighted by the red circles.

points. These segmentation-based CPD algorithms may miss important change points within a segment.

The clustering-based TICC algorithm [Hallac *et al.*, 2017] generates a sparse Gaussian inverse covariance matrix in clustered segments. However, TICC requires defining the number of clustering functions as a hyperparameter, necessitating prior knowledge and limiting the algorithm to detecting only a fixed number of change points. The Gaussian Process (GP) and Bayesian-based ADAGA algorithm [Caldarelli *et al.*, 2022] define both the mean and covariance structure of the temporal process based on the GP kernel. However, ADAGA is sensitive to the GP-kernel type, which also requires prior knowledge. These GP-based CPD algorithms have limitations in capturing non-smoothness, as GP approximates smoothness using mean-square differentiable functions [Banerjee and Gelfand, 2003].

Empirically, Figure 6-(b) highlights the detected change points specifically in the mean shift on the ETTh1 dataset across different CPD algorithms. In general, as depicted in Figure 6-(c), probabilistic-based CPD algorithms exhibit a notable limitation by primarily detecting mid-points (green) in mean shifts rather than the vertices of abrupt changes (red), which are solely due to variance perturbations. This limitation leads to an over-smoothing issue in trend extraction, as further illustrated in Figure 7-(b) and -(c).

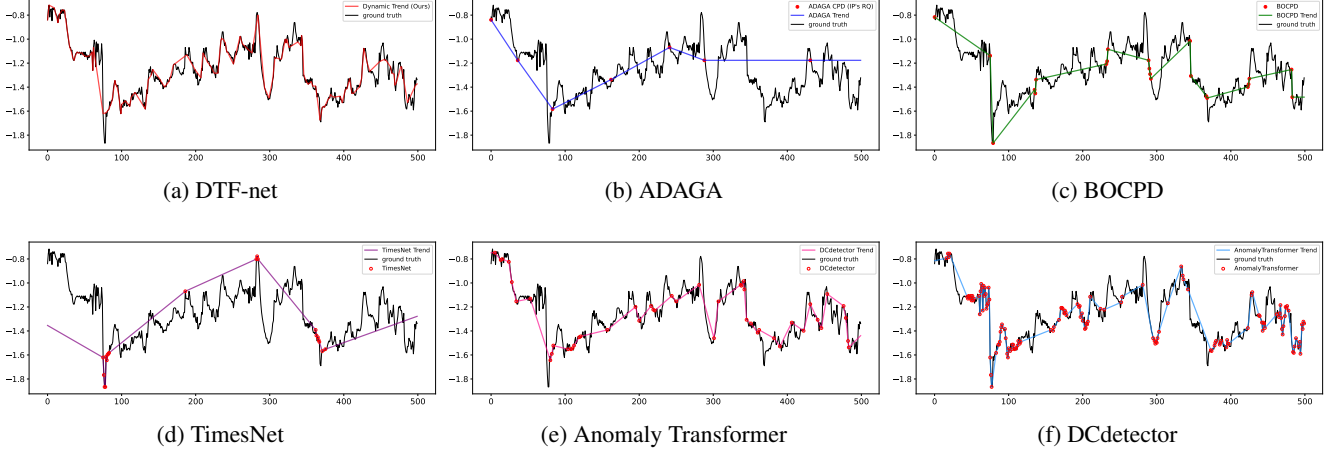


Figure 7: **Limitation of CPD and anomaly detection algorithms in trend filtering.** The figure presents comparative experiments involving DTF-net, CPD, and Anomaly Detection for trend filtering on the ETTh1 dataset. CPD algorithms excel in capturing change points related to mean shifts but face challenges when dealing with points exhibiting variance shifts. While anomaly detection methods prioritize extreme values over CPD, they focus solely on abnormal points and lack the ability to detect midpoints that are crucial for reflecting trends. In contrast, DTF-net dynamically performs trend filtering by incorporating abrupt changes, as exemplified around the 300th point.

A.2 Anomaly Detection

Anomaly detection involves identifying abnormal points or sub-sequences distinguished from the regular patterns found in the majority of the dataset. As the goal of capturing extreme values aligns with DTF-net’s objectives, we conduct a comparison with advanced anomaly detection algorithms, including TimesNet [Wu *et al.*, 2023], Anomaly Transformer [Xu *et al.*, 2022], and DCdetector [Yang *et al.*, 2023].

TimesNet [Wu *et al.*, 2023] utilizes a Temporal Variation Modeling methodology, which is a transforming technique of the original 1D time series into a 2D space to capture multi-periodicity and complex interactions in time series data. However, due to its focus on complex patterns, TimesNet tends to predict extreme anomaly points and might not perform optimally in trend filtering tasks, as illustrated in Figure 7-(d). Anomaly Transformer [Xu *et al.*, 2022] introduces a novel Anomaly-Attention mechanism, employing a Gaussian kernel and minimax strategy to enhance normal-abnormal distinguishability. Nevertheless, due to the Gaussian kernel’s smoothness, it fails to detect some important peaks at 80, 300, and 350. DCdetector [Yang *et al.*, 2023] adopts a unique dual attention asymmetric design for contrastive learning, creating a permuted environment through patching techniques. Leveraging contrastive learning, the DCdetector exhibits a more generalized architecture compared to the Anomaly Transformer, but it still faces challenges in detecting peaks around 300. Additionally, the trend filtering task faces challenges in smoothing noisy sub-sequences, particularly around axes 70 and 450. All the mentioned anomaly detection algorithms exhibit sensitivity to thresholds, and even with an appropriate threshold, points are often missed in peak regions, such as around 300. In summary, while anomaly detection algorithms often miss crucial mid-points of changes, CPD algorithms may overlook essential change points in variance shifts.

B Extended Related Work on RL

B.1 RL for Discrete Action Space

In Reinforcement Learning (RL), the agent consistently interprets and responds to an environment to maximize a specified reward. The environment is a series of events, prompting the agent to select actions that it deems most conducive to achieving the maximum long-term reward. Within the framework of Markov Decision Processes (MDP), the agent learns optimal actions to enhance the cumulative reward associated with each state. A Markov chain illustrates the relationships among sequences of events, providing crucial information for models designed specifically for time series analysis, where discerning underlying trends is imperative [Geyer, 1992; Sutton and Barto, 2018; Liu *et al.*, 2022a].

The probability distribution that an action is selected for each state is referred to as the policy, denoted as $\pi(A|S) = \Pr(A|S)$. The state-value function, denoted as $v_\pi(S)$, represents the expected return value following policy π from state S and is defined as follows,

$$\begin{aligned} v_\pi(S) &= E_\pi[G|S] = E_\pi[\mathcal{R}' + \gamma v_\pi(S')|S] \\ &= \sum_A \pi(A|S)(\mathcal{R} + \gamma \sum_{S'} \Pr(S'|S, A)v_\pi(S')), \end{aligned} \quad (9)$$

where S' and R' represent the next state and reward, and $G = \sum_{k=0}^{\infty} \gamma^k \mathcal{R}'_k$. The action-value function, denoted as $q_\pi(S, A)$, is the expected value of the return from taking action A in state S :

$$\begin{aligned} q_\pi(S, A) &= E_\pi[G|S, A] \\ &= E_\pi[\mathcal{R}' + \gamma q_\pi(S', A')|S] \\ &= \mathcal{R} + \gamma \sum_{S'} \Pr(S'|S, A) \sum_{A'} \pi(A'|S') q_\pi(A'|S'), \end{aligned} \quad (10)$$

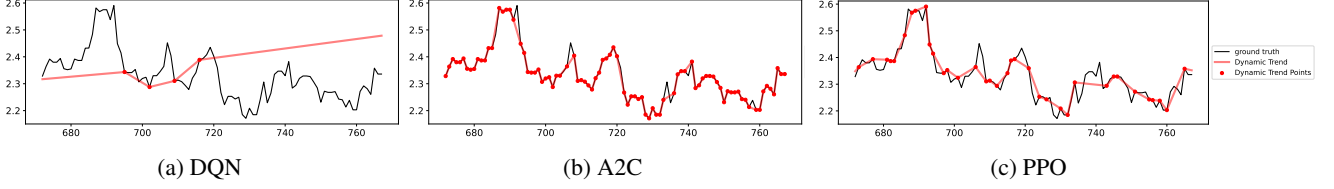


Figure 8: **Dynamic trend filtering with different RL algorithms.** The figure illustrates different trend-filtering outcomes obtained using various RL algorithms. DQN demonstrates an underfitting trend, while A2C exhibits an overfitting trend.

based on the Bellman equation,

$$v_{\pi}(S) = \sum_A \pi(S, A) \sum_{S'} \Pr(S'|S, A) (\mathcal{R} + \gamma v_{\pi}(S')). \quad (11)$$

In model-based RL, the agent constructs an internal model or representation of the environment, requiring state transition probabilities and corresponding rewards for each state. Model-based methods involve dynamic programming or Monte Carlo simulation for planning based on the acquired model. In contrast, model-free RL teaches agents to interact directly with the environment, mapping states to actions without estimating transition dynamics. Model-free methods rely on trial-and-error learning, where the agent explores the environment, receives feedback in the form of rewards, and adjusts its strategy over time based on observed outcomes. Common model-free approaches include Deep Q Networks (DQN) and Policy Gradient methods. In this research, our focus is on model-free approaches.

DQN To address the challenges of applying Q-learning to environments with high-dimensional state spaces, DQN combines Q-learning with DNNs. It uses DNNs to approximate the Q-function, which represents the expected cumulative future rewards for taking an action in a given state. With two separate networks, the Q-network and the target network, DQN stabilizes the learning process by providing fixed targets for Q-values during temporal difference updates. The Q-network is used to select actions, while the target network is periodically updated with the Q-network’s weights. Additionally, with a defined replay buffer, DQN stores past experiences, such as the state, action, reward, and next state of the agent. During training, random batches of experiences are sampled from the replay buffer, breaking the temporal correlation between consecutive samples and improving data efficiency [Mnih *et al.*, 2015].

A2C To overcome the limitation of increasing variance as the episode prolongs, Actor-Critic methods do not use a replay buffer but instead learn actions directly. The Actor-Critic framework defines both an actor and a critic, with the policy network estimating actions and the value function estimating state-action values, respectively. A2C is one such Actor-Critic algorithm that combines elements of both policy iteration (the actor) and value iteration (the critic) to improve stability and sample efficiency. The actor is responsible for selecting actions based on the current policy, while the critic evaluates the value of state-action pairs. Using policy gradients, A2C updates the actor’s policy to maximize the expected cumulative reward. For updating value estimates, A2C

employs temporal difference errors, which represent the difference between the observed return and the current estimate of the value function [Mnih *et al.*, 2016].

PPO Another actor-critic method, PPO, is designed to optimize policies for environments with both continuous and discrete action spaces. It employs a surrogate objective function that combines policy improvement with a clip ratio, controlling the extent of policy updates in each iteration to enhance stability. The clip ratio acts as a trust region constraint, preventing large policy deviations. PPO utilizes policy gradient updates and multiple epochs for training, involving the collection of experiences, computation of policy updates, and application to the policy. Additionally, it often incorporates value function optimization to better estimate state values. Known for its stability and robustness, PPO has been widely applied to diverse tasks, demonstrating effectiveness in both continuous and discrete action environments [Schulman *et al.*, 2017].

B.2 Motivation of Using RL for Trend Filtering

Stock trading represents one of the most representative problems modeled within an MDP using time series data [Liu *et al.*, 2022a]. The decision-making process adheres to the Markov property, where actions depend solely on the immediate preceding state and are not influenced by the past. The optimal trading points are equivalent to abrupt changes and extreme values: buying at the lowest turning point and selling at the highest to maximize profit. To solve this MDP-modeled stock trading problem, RL stands out as one of the most popular methods capable of directly detecting trading points through an agent’s action prediction. Motivated by these equivalences, we formulate the Trend Point Detection problem as an MDP and use RL to solve it, aiming to identify essential points for trend filtering.

B.3 Gaussian Distribution and Reward Function

According to [Kuss and Rasmussen, 2003], in a continuous state space, the Bellman Equation (11) can be generalized by substituting sums with integral when the policy is deterministic:

$$\begin{aligned} v_{\pi}(S) &= \int \Pr(S'|S, \pi(S)) (\mathcal{R}_{\pi(S)} + \gamma v_{\pi}(S')) dS' \\ &= \int \Pr(S'|S, \pi(S)) \mathcal{R}_{\pi(S)} dS' \\ &\quad + \gamma \int \Pr(S'|S, \pi(S)) v_{\pi}(S') dS', \end{aligned} \quad (12)$$

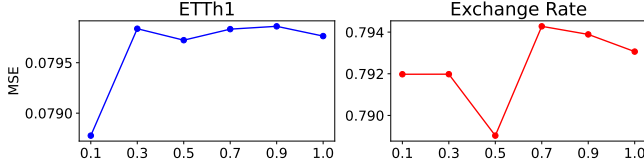


Figure 9: **DTF-net prevents overfitting problems.** The figure illustrates each dataset has an optimal reward sampling ratio while addressing the overfitting issue. The x -axis denotes the reward sampling ratio, while the y -axis represents the MSE.

where $\pi(S)$ is consecutive states S' when following the policy π . Based on Equations (5), (7), the reward is a Gaussian distribution over consecutive state variable S' , where $R_{\pi(S)}$ follows $\mathcal{N}(y_t, \tau^2)$.

Then, policy update is defined as follows,

$$\pi(S) \leftarrow \operatorname{argmax}_A \int \Pr(S'|S, A)(R + \gamma v(S'))dS'. \quad (13)$$

Therefore, the policy is optimized based on the distribution of time series data, following a Gaussian distribution. This allows the agent to predict actions based on time series patterns, enabling different trend point detections in distinct subsequences while capturing temporal dependencies.

B.4 Sampling and Penalty Reward

In RL, positive rewards and penalty rewards are utilized to shape the behavior of the agent by providing feedback on its actions. Positive rewards are assigned to actions that bring the agent closer to the desired goal or enhance its performance, encouraging the agent to repeat those actions. Conversely, penalty rewards are associated with actions that should be avoided or are suboptimal. These penalty rewards discourage the agent from taking undesirable actions, guiding it away from unfavorable behavior. In DTF-net, a penalty reward in the form of a negative sum-of-squares function is employed. However, penalizing at every timestep may cause the agent to become overly fitted to the original time series data, as it aims to minimize the penalty consistently. To address this limitation, a sampling method is employed to determine the penalizing interval, providing a solution to overcome this challenge. We empirically demonstrate that the optimal reward sampling ratio enhances the performance of DTF-net, as shown in Figure 9.

B.5 Computational complexity

While RL for trend filtering enhances dynamic trend extraction and abrupt change capture, it comes with increased computational complexity, rising from $\mathcal{O}(1)$ to $\mathcal{O}(n)$ compared to other trend filtering methods. This increase is due to the batch learning of deep networks in RL, while other methods optimize the entire sequence with a single cost function at once. However, we address this computational inefficiency through three strategies. First, we employ an MLP policy network, which has lower computational costs compared to convolutional or recurrent-based architectures while enhancing trend-filtering performance. Second, we incorporate random sampling in DTF-net for the state and reward, utilizing

only part of the data and not calculating the reward in every step. Third, we keep the episode iteration at less than 10, mitigating the overfitting issue and reducing time complexity simultaneously. Additionally, from the perspective of the data-intensive nature of deep networks, DTF-net demonstrates robust performance with a small number of datasets, such as synthetic or illness data, using a simple MLP policy network. In summary, DTF-net effectively minimizes the increase in computational complexity when applying RL for trend filtering.

C Extended Experiments on TSF

C.1 TSF Dataset

Based on the ADF test, we specifically choose non-stationary datasets in the TSF benchmark to evaluate DTF-net’s ability to capture abrupt changes in Table 2 [Liu *et al.*, 2022b].

Dataset	Variable Number	Sampling Frequency	ADF Test Statistic
Exchange	8	1Day	-1.889
ILI	7	1Week	-5.406
ETT	7	1Hour / 15Minutes	-6.225
Electricity	321	1Hour	-8.483
Traffic	862	1Hour	-15.046
Weather	21	10Minutes	-26.661

Table 3: **Summary of TSF datasets.** A smaller ADF test statistic indicates a more stationary dataset.

ADF Test

The Augmented Dickey-Fuller (ADF) test is a statistical test used to determine whether a unit root is present in a univariate time series dataset. The presence of a unit root indicates that the time series data has a stochastic trend and is non-stationary. The null hypothesis of the ADF test is that a unit root is present, suggesting non-stationarity. If the test statistic is significantly below a critical value, the null hypothesis is rejected, indicating that the time series is stationary after differencing.

The ADF test is conducted using the following regression equation:

$$\Delta y_t = \alpha + \beta t + \gamma y_{t-1} + \delta_1 \Delta y_{t-1} + \dots + \delta_{p-1} \Delta y_{t-p+1} + \epsilon_t,$$

where Δy_t is the differenced series at time t , y_{t-p} is lagged value, t is a time trend variable, δ_i are coefficients on lagged differences terms, and ϵ_t is residual term.

Benchmark Dataset

- **Exchange** dataset comprises daily exchange rates of eight foreign countries, spanning from 1990 to 2016 [Zhou *et al.*, 2021].
- **Illness** dataset includes patient data for influenza illness recorded weekly from the US Centers for Disease Control and Prevention between 2002 and 2021. It represents the ratio of patients seen with influenza-like illness to the total number of patients [Wu *et al.*, 2021].
- **ETT** (Electricity Transformer Temperature) dataset consists of recorded over a one-hour/minute period. Each data point includes the target value ‘Oil Temperature’ along with six power load features [Zhou *et al.*, 2021].
- **Electricity** dataset consumption data, measured in kilowatt-hours (Kwh), was gathered from 312 clients. To account for missing values, the data was converted into hourly consumption over a span of two years [Zhou *et al.*, 2021].
- **Traffic** dataset comprises hourly information from the California Department of Transportation, detailing road occupancy rates measured by various sensors on San Francisco Bay Area freeways [Wu *et al.*, 2021].
- **Weather** dataset includes local climatological data for nearly 1,600 U.S. locations, with data points collected every hour over a span of four years [Zhou *et al.*, 2021].

C.2 TSF Baselines.

TSF Baseline Models

- **Autoformer**, a Transformer-based method, utilizes a decomposition and auto-correlation mechanism based on fast Fourier transform to learn the temporal patterns of time series data [Wu *et al.*, 2021].
- **FEDformer**, a Transformer-based method, introduces a Mixture of Experts (MOE) for seasonal-trend decomposition and utilizes frequency-enhanced block/attention with Fourier and Wavelet Transform [Zhou *et al.*, 2022].
- **DLinear**, relying solely on linear layers, decomposes the original input into trend and remainder components using global average pooling. Two linear layers are applied to each component, and the resulting features are summed up to obtain the final prediction [Zeng *et al.*, 2023].
- **NLinear** employs a straightforward normalization technique to tackle the train-test distribution shift in the dataset. This technique involves subtracting the last value from the input and adding it back before making the final prediction, all while using only a single linear layer [Zeng *et al.*, 2023].
- **PatchTST**, a transformer-based method, comprises two components: the segmentation of time series into subseries-level patches and a channel-independent structure. PatchTST can capture local semantic information and benefits from longer look-back windows, utilizing patching techniques [Nie *et al.*, 2023].

Hyper-parameters

Dataset	Input Length	Prediction Length	Forecasting Model	Reward Ratio	Learning Rate	RL Steps	Forecasting Epoch	Max Sequence Length
Exchange Rate	336	720	DLinear	0.4	5e-4	10000	15	3000
	336	336	DLinear	0.4	5e-4	10000	15	3000
	336	192	DLinear	0.4	1e-4	10000	15	3000
	336	96	NLinear	0.4	1e-4	3000	15	3000
	336	48	NLinear	0.4	1e-4	3000	15	3000
	336	24	NLinear	0.4	1e-4	3000	15	3000
ETTh1	336	720	NLinear	0.1	1e-3	10000	20	3000
	336	336	NLinear	0.1	9e-4	10000	15	3000
	336	192	NLinear	0.1	3e-4	10000	15	3000
	336	96	NLinear	0.1	5e-4	1000	15	3000
	336	48	NLinear	0.1	5e-4	1000	15	3000
	336	24	NLinear	0.1	5e-4	1000	15	3000
Illness	104	60	NLinear	0.1	1e-3	1000	15	300
	104	48	NLinear	0.1	1e-3	5000	15	300
	104	24	NLinear	0.1	1e-3	10000	15	300

Table 4: **Hyper-Parameters.**

The experiments are conducted under the same conditions, employing the Adam optimizer, MSE loss function, 15 epochs, and batch sizes of 32. The input sequence length for linear models is set to 336, while Transformer models utilize an optimal length of 96. The learning rate for the baseline model follows the values outlined in Table 4, and in cases of overfitting, it is adjusted to $1e - 4$. The seed number is arbitrarily set to 2023.

C.3 Dynamic Trend Extraction of DTF-net

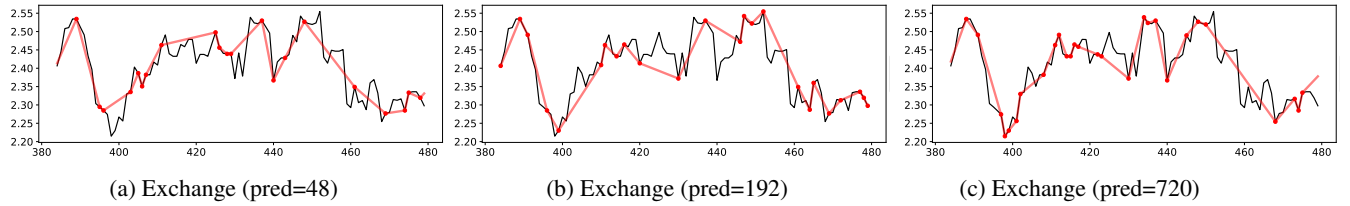


Figure 10: **Dynamic trend filtering of DTF-net with different prediction length.** The figure demonstrates that DTF-net extracts various trends based on different prediction horizon lengths on the Exchange Rate Dataset.

In comparison to traditional trend filtering methods, DTF-net extracts dynamic trends with varying levels of smoothness for each sub-sequence. This is achievable by adjusting the prediction length, as shown in Figure 10.

D Extended Ablation Study on DTF-net

D.1 Ablation Study on State

State	Episode length	non-sequential dynamic		non-sequential static		sequential dynamic		sequential static		zero padding	
Metric		MSE	MAE	MSE	MAE	MSE	MAE	MSE	MAE	MSE	MAE
Exchange	24	0.0250	0.1198	0.0263	0.1228	0.0264	0.1231	<u>0.0263</u>	<u>0.1227</u>	0.0259	0.1215
	48	0.0487	0.1658	0.0500	0.1697	<u>0.0496</u>	0.1689	0.0501	0.1699	0.0486	0.1655
	96	<u>0.0983</u>	<u>0.2349</u>	0.0995	0.2363	<u>0.0994</u>	<u>0.2363</u>	0.0982	0.2348	0.0983	0.2350
	192	0.1983	0.3583	0.1986	0.3587	0.2013	0.3607	<u>0.1984</u>	<u>0.3582</u>	0.2003	0.3598
	336	<u>0.3160</u>	<u>0.4561</u>	0.3163	0.4562	0.3166	0.4562	0.3140	0.4541	0.3166	0.4564
	720	<u>0.7933</u>	<u>0.6874</u>	0.7922	0.6822	<u>0.7903</u>	0.6878	0.7893	<u>0.6874</u>	0.7889	0.6871
ETTh1	24	0.0253	0.1205	0.0264	0.1228	<u>0.0255</u>	<u>0.1205</u>	0.0259	0.1214	0.0258	0.1216
	48	0.0375	<u>0.1479</u>	0.0381	0.1487	0.0381	0.1485	<u>0.0379</u>	0.1478	0.0379	0.1479
	96	0.0519	0.1740	0.0551	0.1810	0.0554	0.1808	<u>0.0553</u>	<u>0.1808</u>	0.0555	0.1811
	192	0.0676	0.2013	<u>0.0680</u>	<u>0.2019</u>	0.0700	0.2051	0.0687	0.2026	0.0695	0.2041
	336	<u>0.0803</u>	<u>0.2247</u>	0.0805	0.2252	0.0796	0.2238	0.0806	0.2254	0.0803	0.2244
	720	0.0776	0.2224	<u>0.0808</u>	<u>0.2271</u>	0.0809	0.2273	0.0808	0.2273	0.0795	0.2255
Illness	24	0.5881	0.5358	<u>0.5805</u>	<u>0.5363</u>	0.5845	0.5376	0.5621	0.5316	0.5808	0.5464
	48	0.6858	0.6359	<u>0.6558</u>	<u>0.6329</u>	0.6813	0.6535	0.6255	0.5964	0.6551	0.6310
	60	<u>0.6640</u>	<u>0.6423</u>	0.7481	0.7029	0.6506	0.6265	0.7455	0.6979	0.6513	0.6270

Table 5: **State ablation study.** The table shows the forecasting performance across different episode progressions (non-sequential vs sequential), episode lengths (dynamic vs static), and state encodings (positional encoding vs zero padding). The best performance is highlighted in **bold**, while the second-best performance is underlined. Additionally, for the comparison between positional encoding and zero padding, the outperformed performance of zero padding is highlighted.

We conduct an ablation study on episode progression and state encoding. First, the progression of the episode is divided into two approaches: a non-sequential approach based on random sampling and a sequential approach following the conventional time axis order. Next, the composition of episode length is categorized into a dynamic approach with random sampling and a static approach using a fixed window. Note that the static length is set to 1500 for Exchange and ETTh1, and 200 for Illness. As shown in Table ‘State’, it is evident that the non-sequential episodes with dynamic length exhibit robust performance. Following this, the traditional approach, sequential episodes with static length, shows the second most robust performance. This confirms that DTF-net achieves the best performance while preventing overfitting issues, in contrast to the sequential episode with static length method that exhibits overfitted results.

Next, positional encoding achieves superior performance compared to zero padding, except for the Illness dataset. For the Illness dataset, zero padding performs better due to its relatively short look-back horizon of 104, making simple zero padding more effective compared to Exchange and ETTh. However, as the look-back horizon for forecasting increases, reaching 336 in Exchange and ETTh1, positional encoding proves to be more effective.

D.2 Ablation Study on Reward with Seed Test

Seed	2023		52		454		470		515		695		1561		1765		1953		2021		2022		
Metric	MSE	MAE	MSE	MAE	MSE	MAE	MSE	MAE	MSE	MAE	MSE	MAE	MSE	MAE	MSE	MAE	MSE	MAE	MSE	MAE	MSE	MAE	
Exchange	24	0.0250	0.1198	0.0265	0.1236	0.0256	0.1211	0.0256	0.1220	0.0258	0.1209	0.0267	0.1237	0.0261	0.1226	0.0253	0.1203	0.0267	0.1239	0.0263	0.1227	0.0265	0.1231
	48	0.0487	0.1658	0.0499	0.1682	0.0498	0.1677	0.0503	0.1691	0.0492	0.1658	0.0492	0.1674	0.0500	0.1681	0.0480	0.1655	0.0493	0.1680	0.0480	0.1650	0.0510	0.1703
	96	0.0983	0.2349	0.1007	0.2363	0.0989	0.2349	0.0970	0.2322	0.0985	0.2322	0.0982	0.2356	0.0992	0.2354	0.0994	0.2360	0.0982	0.2350	0.1007	0.2335	0.1004	0.2368
	192	0.1983	0.3583	0.2096	0.3673	0.2004	0.3562	0.2023	0.3565	0.2115	0.3751	0.2009	0.3567	0.1978	0.3595	0.2063	0.3667	0.1904	0.3513	0.2056	0.3649	0.1929	0.3512
	336	0.3160	0.4561	0.4085	0.4939	0.3311	0.4712	0.3288	0.4678	0.3409	0.4716	0.3180	0.4467	0.3199	0.4587	0.3559	0.4874	0.3333	0.4626	0.3124	0.4578	0.3606	0.4768
720	0.7933	0.6874	0.7583	0.6847	0.8022	0.7083	0.8888	0.7331	1.0462	0.7928	0.9455	0.7649	0.9338	0.7445	1.0001	0.7788	0.8769	0.8769	0.9480	0.7534	0.7889	0.6985	
ETTh1	24	0.0253	0.1205	0.0258	0.1219	0.0259	0.1218	0.0266	0.1234	0.0259	0.1222	0.0250	0.1197	0.0261	0.1224	0.0264	0.1235	0.0263	0.1233	0.0258	0.1214	0.0260	0.1221
	48	0.0375	0.1479	0.0381	0.1485	0.0383	0.1489	0.0388	0.1501	0.0404	0.1546	0.0388	0.1497	0.0391	0.1507	0.0389	0.1505	0.0370	0.1467	0.0391	0.1508	0.0386	0.1490
	96	0.0519	0.1740	0.0528	0.1763	0.0561	0.1824	0.0532	0.1774	0.0536	0.1774	0.0540	0.1780	0.0544	0.1789	0.0525	0.1755	0.0531	0.1768	0.0539	0.1777	0.0536	0.1783
	192	0.0676	0.2013	0.0697	0.2041	0.0683	0.2036	0.0704	0.2057	0.0698	0.2048	0.0703	0.2054	0.0681	0.2024	0.0695	0.2034	0.0695	0.2049	0.0694	0.2044	0.0686	0.2032
	336	0.0803	0.2247	0.0856	0.2325	0.0781	0.2231	0.0818	0.2272	0.0834	0.2285	0.0833	0.2291	0.0801	0.2247	0.0792	0.2232	0.0815	0.2266	0.0819	0.2278	0.0807	0.2253
720	0.0776	0.2224	0.0784	0.2239	0.0823	0.2288	0.0820	0.2285	0.0832	0.2304	0.0820	0.2278	0.0813	0.2278	0.0814	0.2282	0.0792	0.2255	0.0802	0.2252	0.0805	0.2262	
Illness	24	0.5881	0.5358	0.6275	0.5617	0.6100	0.5498	0.6684	0.5718	0.6285	0.5689	0.5647	0.5117	0.5764	0.5310	0.6112	0.5424	0.5476	0.5303	0.7151	0.6080	0.6570	0.5621
	48	0.6858	0.6359	0.7178	0.6531	0.6534	0.6170	0.7407	0.6822	0.7241	0.6626	0.5881	0.5655	0.6829	0.6604	0.6343	0.6021	0.5991	0.5642	0.7104	0.6532	0.7159	0.6435
	60	0.6640	0.6423	0.6682	0.6448	0.7822	0.7338	0.7314	0.6879	0.6492	0.6290	0.7194	0.6805	0.7020	0.6607	0.6526	0.6399	0.7493	0.6955	0.6769	0.6408	0.6479	0.6196
var / length		24	48	60	96	192	336	720															
Exchange		3e-7	9e-7	-	1e-6	5e-5	8e-4	9e-3															
ETTh1		1e-7	7e-7	-	1e-6	6e-7	5e-6	2e-6															
Illness		3e-3	3e-3	2e-3	-	-	-	-															

Table 6: **Equal interval reward sampling.** The table presents the forecasting performance across different seeds with rewards sampled at equal intervals. Results from the seed that demonstrated superior performance, using the 2023 seed with a random interval as the reference result, are highlighted in **bold**. The second table illustrates the performance variance of the seed tests based on MSE.

Seed		2023		52		454		470		515		695		1561		1765		1953		2021		2022	
Metric		MSE	MAE	MSE	MAE	MSE	MAE	MSE	MAE	MSE	MAE	MSE	MAE	MSE	MAE	MSE	MAE	MSE	MAE	MSE	MAE	MSE	MAE
Exchange	24	0.0250	0.1198	0.0265	0.1237	0.0251	0.1198	0.0259	0.1228	0.0250	0.1186	0.0254	0.1207	0.0254	0.1205	0.0257	0.1210	0.0269	0.1244	0.0263	0.1230	0.0261	0.1218
	48	0.0487	0.1658	0.0491	0.1666	0.0498	0.1678	0.0502	0.1682	0.0492	0.1658	0.0491	0.1665	0.0497	0.1670	0.0479	0.1652	0.0495	0.1682	0.0485	0.1665	0.0498	0.1683
	96	0.0983	0.2349	0.1003	0.2356	0.1009	0.2348	0.0970	0.2322	0.0968	0.2308	0.0952	0.2323	0.0985	0.2345	0.0991	0.2355	0.0996	0.2366	0.1006	0.2343	0.1004	0.2366
	192	0.1983	0.3583	0.2091	0.3652	0.2019	0.3575	0.1994	0.3538	0.2130	0.3760	0.2028	0.3579	0.1990	0.3593	0.2093	0.3693	0.1907	0.3515	0.2055	0.3648	0.1924	0.3508
	336	0.3160	0.4561	0.4040	0.4926	0.3329	0.4728	0.3284	0.4675	0.3409	0.4719	0.3202	0.4480	0.3193	0.4581	0.3571	0.4880	0.3334	0.4629	0.3122	0.4585	0.3638	0.3638
	720	0.7933	0.6874	0.7600	0.6855	0.7693	0.6920	0.8888	0.7332	1.0404	0.7913	0.9442	0.7636	0.9398	0.7483	0.9857	0.7745	0.8746	0.7249	0.9457	0.7529	0.7856	0.6955
ETTh1	24	0.0253	0.1205	0.0257	0.1214	0.0258	0.1218	0.0268	0.1235	0.0257	0.1218	0.0250	0.1196	0.0261	0.1225	0.0260	0.1222	0.0254	0.1203	0.0258	0.1215	0.0261	0.1222
	48	0.0375	0.1479	0.0381	0.1485	0.0386	0.1493	0.0396	0.1513	0.0378	0.1488	0.0389	0.1499	0.0391	0.1506	0.0387	0.1502	0.0370	0.1470	0.0388	0.1502	0.0385	0.1490
	96	0.0519	0.1740	0.0529	0.1765	0.0557	0.1819	0.0535	0.1779	0.0537	0.1778	0.0525	0.1751	0.0543	0.1789	0.0526	0.1757	0.0525	0.1760	0.0538	0.1774	0.0536	0.1783
	192	0.0676	0.2013	0.0698	0.2040	0.0709	0.2067	0.0717	0.2081	0.0698	0.2049	0.0697	0.2046	0.0680	0.2023	0.0696	0.2034	0.0703	0.2063	0.0695	0.2042	0.0690	0.2040
	336	0.0803	0.2247	0.0845	0.2314	0.0783	0.2229	0.0818	0.2272	0.0825	0.2277	0.0844	0.2302	0.0800	0.2251	0.0822	0.2268	0.0806	0.2256	0.0820	0.2271	0.0807	0.2250
	720	0.0776	0.2224	0.0782	0.2234	0.0808	0.2267	0.0826	0.2292	0.0823	0.2292	0.0790	0.2237	0.0808	0.2272	0.0801	0.2253	0.0805	0.2271	0.0804	0.2254	0.0800	0.2253
Illness	24	0.5881	0.5358	0.6157	0.5495	0.6326	0.5689	0.6237	0.5672	0.7393	0.6669	0.6341	0.5293	0.6009	0.5684	0.6278	0.5575	0.6121	0.5471	0.6330	0.5590	0.6681	0.5958
	48	0.6858	0.6359	0.7181	0.6537	0.7076	0.6407	0.7800	0.7061	0.7205	0.6726	0.6598	0.5907	0.6958	0.6621	0.6363	0.6025	0.6254	0.5743	0.6340	0.6171	0.7155	0.6495
	60	0.6640	0.6423	0.6542	0.6329	0.7767	0.7326	0.7394	0.6881	0.6728	0.6501	0.7359	0.6929	0.7140	0.6658	0.6626	0.6460	0.7291	0.6829	0.6598	0.6236	0.6483	0.6203
var / length		24	48	60	96	192	336	720															
Exchange		4e-7	5e-7	-	4e-7	5e-7	8e-4	9e-3															
ETTh1		2e-7	5e-7	-	1e-6	1e-6	4e-6	2e-6															
Illness		2e-3	3e-3	2e-3	-	-	-	-															

Table 7: **Random interval reward sampling.** The table presents the forecasting performance across different seeds with rewards sampled at random intervals. Results from the seed that demonstrated superior performance, using the 2023 seed with a random interval as the reference result, are highlighted in **bold**. The second table illustrates the performance variance of the seed tests based on MSE.

We conduct experiments under two conditions to assess the performance of DTF-net using different reward sampling methods with 10 randomly selected seeds: 1) sampling rewards at equal intervals (Table 6), and 2) sampling rewards at random intervals (Table 7). As shown in the tables, there are no significant disparities between the two interval reward sampling methods. However, concerning the seed test, as the prediction horizon increases, the variance of performance of the seed test also increases. This limitation is inherent to RL's sensitivity to hyperparameters, including seeds. Nevertheless, it is important to note that this sensitivity can also be advantageous, as optimal performance can be achieved by identifying the appropriate combination of hyperparameters.

E Limitation of DTF-net

E.1 DTF-net on Stationary TSF: Weather and Traffic Dataset

Methods		DTF-Linear (ours)		$\ell_1(\lambda = 0.1)$ -Linear		NLinear		DLinear		FEDformer-f		FEDformer-w		Autoformer	
Metric		MSE	MAE	MSE	MAE	MSE	MAE	MSE	MAE	MSE	MAE	MSE	MAE	MSE	MAE
Weather	24	0.0004	0.0143	0.0004	0.0133	<u>0.0004</u>	<u>0.0128</u>	0.0019	0.0323	0.0272	0.1263	0.0217	0.0217	0.0133	0.0957
	48	0.0008	0.0208	<u>0.0008</u>	<u>0.0188</u>	<u>0.0007</u>	<u>0.0190</u>	0.0043	0.0513	0.0053	0.0586	0.0055	0.0599	0.0115	0.0850
	96	0.0010	0.0236	<u>0.0010</u>	<u>0.0227</u>	<u>0.0010</u>	<u>0.0233</u>	0.0047	0.0543	0.0096	0.0770	0.0055	0.0593	0.0094	0.0769
	192	0.0012	0.0253	0.0012	0.0257	<u>0.0012</u>	<u>0.0261</u>	0.0054	0.0591	0.0048	0.0558	0.0048	0.0559	0.0055	0.0570
	336	0.0014	0.0277	0.0014	0.0279	<u>0.0014</u>	<u>0.0278</u>	0.0064	0.0664	0.0049	0.0554	0.0049	0.0552	0.0082	0.0683
	720	0.0019	0.0318	0.0019	0.0323	<u>0.0019</u>	<u>0.0329</u>	0.0066	0.0679	0.0036	0.0479	0.0036	0.0478	0.0055	0.0561
Traffic	24	0.1155	0.1963	0.1248	0.2174	0.1159	<u>0.1962</u>	0.1166	0.1986	0.1526	0.2535	0.1506	0.2432	0.2279	0.3461
	48	0.1251	0.2110	0.1327	0.2240	<u>0.1214</u>	<u>0.2002</u>	0.1228	0.3505	0.1729	0.2772	0.1803	0.2759	0.2523	0.3666
	96	0.1391	0.2283	0.1402	0.2322	<u>0.1282</u>	<u>0.2074</u>	0.1300	0.2114	0.1890	0.2884	0.1933	0.2872	0.2550	0.3665
	192	0.1389	0.2263	0.1429	0.2354	<u>0.1328</u>	<u>0.2132</u>	0.1331	0.2151	0.1901	0.2936	0.1955	0.2978	0.2531	0.3594
	336	0.1619	0.2629	0.1419	0.2377	<u>0.1301</u>	<u>0.2163</u>	0.1331	0.2213	0.1980	0.3073	0.2000	0.3092	0.2965	0.3926
	720	0.1548	0.2518	0.1550	0.2516	<u>0.1423</u>	<u>0.2283</u>	0.1455	0.2349	0.2601	0.3469	0.2634	0.3474	0.3935	0.4562

Table 8: **DTF-net on stationary TSF.** We conduct TSF experiments using two stationary datasets: Weather and Traffic. Performance is evaluated using MSE and MAE, where lower values indicate better performance. In the following results, the best-performing models using DTF-net are highlighted in **bold**, and models using ℓ_1 trend filtering are highlighted in *italic*. To compare the results, the best-performing models using the original data are underlined.

DTF-net is specifically designed to tackle the trend filtering problem, focusing on capturing abrupt changes driven by extreme values. Therefore, DTF-net may not be the most suitable choice for handling stationary datasets. To support this assertion, we observe that both DTF-net and ℓ_1 trend filtering exhibit suboptimal performance in terms of TSF when applied to stationary datasets. This suggests that the emphasis on trend filtering, particularly in capturing abrupt changes, may impact the performance of TSF negatively. Nevertheless, as indicated by the results in Table 2 and Figure 5, we substantiate that DTF-net significantly improves TSF performance when dealing with non-stationary and complex datasets.

E.2 Multivariate Trend Filtering and Time Series Forecasting

DTF-net is employed for univariate trend filtering on features derived from multivariate time series data. In this context, RL leverages multidimensional aspects to perform trend filtering specifically on the target variable. It’s worth noting that this study does not explicitly address multivariate trend filtering for all dimensions within the time series data. However, we believe that achieving this is feasible through the multi-discrete action prediction capability of the PPO algorithm [Schulman *et al.*, 2017].

E.3 Stability of DTF-net

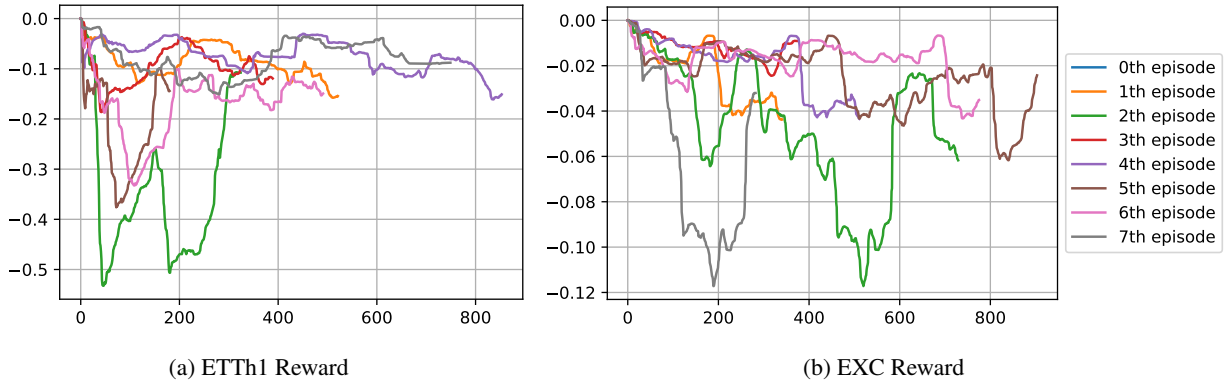


Figure 11: The figure shows rewards obtained from dynamically segmented sub-sequences across different episodes from ETTh1 and Exchange Rate (EXC). Since DTF-net uses the forecasting cost function as a reward, the reward tends to be unstable.

Regarding stability and convergence, in each episode, there is a tendency for cumulative reward to increase, but due to the nature of forecasting MSE, the reward can be unstable depending on the characteristics of the input data batch. While acknowledging the degradation in complexity and stability, DTF-net demonstrates clear advantages in extracting dynamic trends.